

## ENGINEERED SUBSTRATES FOR THIN-FILM SOLAR CELLS: SCATTERING PROPERTIES OF 1D ROUGHNESS

S. Del Sorbo<sup>1\*</sup>, P. Kowalczewski<sup>1</sup>, S. Pirotta<sup>1</sup>, M. Galli<sup>1</sup>, L. C. Andreani<sup>1</sup>, C. Mennucci<sup>2</sup>, C. Martella<sup>2</sup>,  
M. C. Giordano<sup>2</sup>, F. Buatier de Mongeot<sup>2</sup>, L. V. Mercaldo<sup>3</sup>, P. Delli Veneri<sup>3</sup>

<sup>1</sup>Department of Physics, University of Pavia, Via Bassi 6, I-27100 Pavia, Italy

<sup>2</sup>Department of Physics, University of Genova, Via Dodecaneso 33, I-16146 Genova, Italy

<sup>3</sup>ENEA Portici Research Center, Piazzale E. Fermi, I-80055 Portici (NA), Italy

\*E-mail: salvatore.delsorbo01@ateneopv.it

**ABSTRACT:** The key advantage of a thin absorbing layer in solar cells is related to reduced electrical transport losses. Yet, decreasing the absorber thickness significantly reduces absorption of sunlight. In this regard, engineering the geometry of substrate allows one to trap the light within a physically thin layer and to maximize the absorption. In this work, we experimentally investigate the scattering properties of one-dimensional rough substrates that provide strong and broad-band absorption enhancement. We demonstrate that these substrates have superior scattering properties with respect to the commonly used Asahi-U textures. In particular, we focus on Angular Resolved Scattering (ARS) and haze of the light transmitted through the rough texture.

**Keywords:** Light Trapping, Optical Properties, Substrates, Texturisation, Thin Film Solar Cells

### 1 MOTIVATION OF THIS WORK

The aim of thin film technology is to reduce both the electrical transport losses in the bulk region of a solar cell (SC) and the amount of material used for the absorber. To achieve this goal, it is necessary to significantly decrease the absorber thickness. Yet, thin-film SCs without a light-trapping scheme suffer from poor absorption. Therefore, light trapping structures are required. In this regard, a study of appropriate substrates for the growth is necessary for the development of thin-film SCs. The target of this kind of studies is to find new geometries of substrates that allow to maximize the light path and absorption within the physically thin layer.

In this work, we perform an optical investigation of a deep textured substrate prepared by surface patterning with defocused ion beams. This substrate is potentially superior to Asahi-U textured glass that is commonly used as a substrate for deposition of thin-film SCs.

In the following sections, we show the study of the scattering properties of these novel rough substrates, which provide strong and broad-band scattering. In particular, we have measured the Angular Resolved Scattering (ARS) and haze (i.e., the ratio of the intensity of scattered light to the total intensity of the light transmitted through the texture) of transmitted light. Finally, we compare our results with the same measurements performed for the Asahi-U texture.

### 2 SAMPLE UNDER INVESTIGATION

The sample studied in this work is a nanostructured glass substrate thought to realize light trapping in thin-film SCs. The absorber layer is conformally grown on the roughness. The resulting texture works as a strong anisotropic front light scatterer for the absorber [1]. The presence of deep structures results in a pseudo-periodic one-dimensional texture (see Fig. 1).

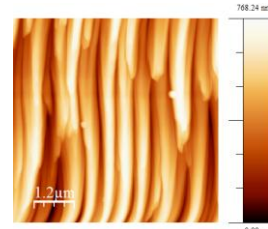


**Figure 1:** AFM image of the nanostructured surface. The color scale indicates the height of the structure. The image shows the quasi-one dimensional character of the surface roughness, as well as its relatively high aspect ratio.

#### 2.1 Fabrication method

The samples under investigation in this work have been prepared in the laboratories of the University of Genova. The fabrication process consists of a self-organized approach based on defocused ion beam sputtering. It starts from a flat glass coated with a polycrystalline gold film (see Fig. 2). A low energy Ar<sup>+</sup> ion beam impinges at grazing incidence angle (82 deg off-normal) on the surface of the Au film. Under ion beam, the gold develops a nanoscale rippled pattern oriented along the ion beam projection. Prolonging further ion bombardment, the metallic ripples form an array of disconnected nanowires, which act as a sacrificial stencil mask for patterning the underlying glass substrate.

This technique allows a one-dimensional roughness induced on a coating to propagate and to amplify the texture on the surface of the destination substrate [1].

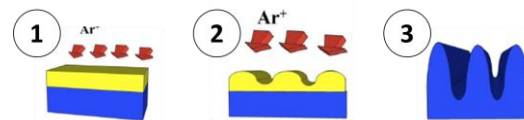


**Figure 2:** Fabrication process of substrate schematized in three fundamental steps; from left to right: 1) it starts from a flat glass coated with a polycrystalline Au film; 2) a low energy defocused Ar<sup>+</sup> beam erodes the Au film crating a stencil mask; 3) under ion beam, this sacrificial mask propagates in the form of a one-dimensional texture on the glass surface.

## 2.2 Texturing of sample surface

As a result of this bottom-up process of texturing, after the complete erosion of the stencil mask, one observes one-dimensional nano-ridges at the glass interface (see Fig. 1). Usually, this type of pseudo-periodic or quasi-random texture is described by two statistical parameters: the root-mean square (RMS) and the lateral correlation length of the heights of roughness. In the case of this fabrication technique, the samples show a lateral correlation length around 200 nm, while the RMS height deviation reaches up to 150 nm. In particular, the sample realized in this work has been engineered to obtain three different regions, each characterized by a different RMS value (see Fig. 3): Zone1 is almost flat, Zone2 has the highest RMS (150 nm), and Zone3 has an intermediate value of RMS (100 nm). This differentiation allows us to correlate the scattering properties to the RMS of the texture.

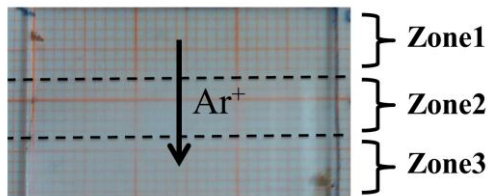


**Figure 3:** Image of the sample studied in this work. The dimensions are 3 cm x 2 cm. RMS of the texture changes in the direction parallel to the  $Ar^+$  flux.

## 3 LIGHT SCATTERING CHARACTERIZATION

In this section, we present the characterization of the scattering properties of the sample described above. The aim is to correlate the scattering functions to the physical features of the texture.

We have measured the angular-resolved scattering (ARS), namely the angular distribution of light scattered in transmission, on the three different regions of glass interface. Then, we have compared the ARS curves with the cosine distribution, which represents the theoretical limit of a Lambertian scatterer [2]. Moreover, we have measured the global scattering power in transmission related to the best region of the sample by determining the haze.

In order to have a reliable comparison with a well-known system, we have characterized in the same manner a common Asahi-U substrate, consisting of a textured glass with deposited  $SnO_2$  layer.

### 3.1 Experimental setup for ARS

In the experiment for measuring the ARS, unpolarized white laser light is shined normally on a flat side of the substrate under investigation (see Fig. 4). The size of the beam is fixed around 2 mm using a diaphragm. The light is scattered by the textured glass-air interface, which is placed in the center of rotation of the collection arm. The scattered light is collected at the various angles by a system of lenses, which focuses it in an optical fiber. This latter drives the optical signal to the detector, which is either a spectrometer or a powermeter with a pass band filter. All control and measurement processes are automatized by a step scanning procedure.

The light source in the experiment is a FIANIUM

super-continuum laser, which provides an almost white light on all the range of wavelengths between 200 and 2000 nm. In the range of interest from 450 nm to 900 nm, the maximum variation in the spectral power is around of a factor of four. This kind of light source combines the advantage of a lamp, yielding a wide white-light spectrum, and that of a laser, giving a highly collimated and coherent light beam. Moreover the super-continuum is speckle-noise free. For the silicon-based photovoltaic systems, the interesting spectral range is in the visible and NIR regions of wavelength. The undesired infrared components of super-continuum spectrum are cut-off by a pass-band filter.

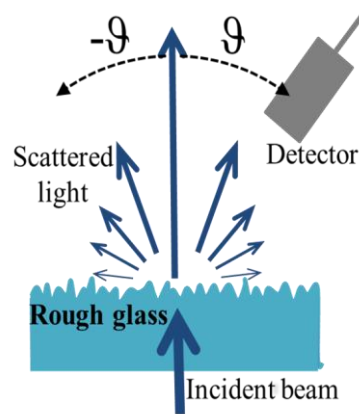


**Figure 4:** Scheme of the experiment. The incident light beam shines on the flat surface of the sample and is scattered by the texture present on the other interface. The transmitted light is collected at various scattering angles (from  $-90$  deg to  $90$  deg) by the detector, which is placed on a rotating arm.

### 3.2 Angular resolved scattering measurements

In this work, we have measured the scattered light in transmission. For our sample, we choose to collect the light in the plane orthogonal to the ripples of the one-dimensional texture. On the other hand, the collection plane does not matter for the Asahi-U sample, because of the isotropy of texture.

The ARS curves measured on the three different regions of the sample and on the Asahi-U texture at a wavelength  $\lambda=600$  nm are shown together in Fig. 5. The measured intensity of the scattered light is plotted as a function of the scattering angle. Since we are interested in the angular trend of scattered light, the ARS is measured by a spectrometer with a CCD detector. This detector captures the information of intensity at fixed scattering angle in the whole spectral range at the same time. On the other hand, it does not allow to follow a variation of signal intensity larger than one order of magnitude. Therefore, in Fig. 5, we plot the data divided by the maximum value of ARS measured in the range of angles from 1 deg to 90 deg (the angular step is 1 deg). Notice that the value measured at 0 deg is set to zero, because it contains the specular component of transmitted light and it is of no importance for the study of angular trend of scattered light. In order to make a comparison with the theoretical trend of the Lambertian scatterer [2], we plot the cosine function in the same graph (dashed line in Fig. 5).

Looking at the graph in Fig. 5, we observe a broadening of ARS with increasing RMS roughness, which is equal

to 150 nm in Zone2, 100 nm in Zone3, and 40 nm for SnO<sub>2</sub> Asahi-U texture. Interestingly, ARS related to Zone2 exhibits a wide peak located between 20 and 30 deg. This peak overcomes the cosine distribution corresponding to the Lambertian scatterer [2]. On the other hand, the other investigated textures have a more regular trend in the ARS curve. We observed a similar behavior in the whole investigated range (between 450 nm and 900 nm).

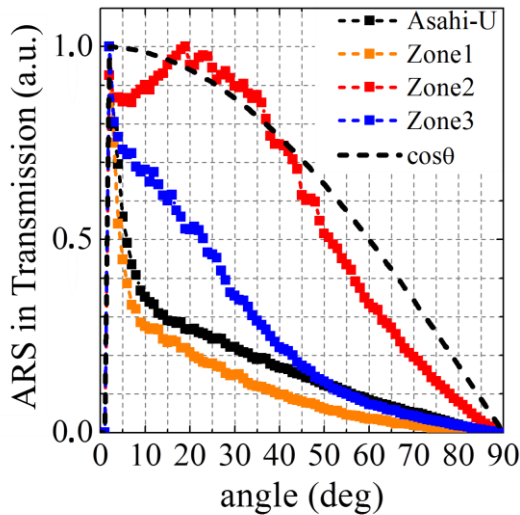


**Figure 5:** The graph of ARS in transmission at wavelength equal to 600 nm. The data represent the intensity of light plotted as a function of scattering angle. The data were divided by the maximum value measured between 1 deg and 90 deg in order to study the angular trend of scattering. The red curve is obtained on Zone 2 of the rough sample, with 150 nm RMS of texturing. The blue curve is on Zone3, with 100 nm RMS. The black curve on Asahi-U with 40 nm RMS. The dashed line is the cosine function, corresponding to the theoretical definition of the Lambertian scatterer. Interestingly, we observe that the scattering in Zone2 (red curve) overcomes the Lambertian scatterer (dash curve) with a wide peak between about 20 and 40 deg.

In the graph shown in Fig. 6, we present the ARS in transmission at 600 nm wavelength. In this case, we are interested in comparing the effective intensity of light scattered by texture in Zone2 with scattering from the Asahi-U substrate. For this reason, the measurement was done with the powermeter. In fact, this instrument allows measuring the real power of collected light at specific wavelengths. The wavelength of interest is selected by inserting a pass-band filter at 600 nm wavelength with 10 nm FWHM before the optical fiber. Moreover, the powermeter follows the change in the light power over several orders of magnitude, without the need to change the acquisition parameters. That allows to measure the ARS on all directions, including the specular one.

The curves plotted in Fig. 6 were obtained by dividing the power measured at the scattering angle by the power measured for the incident beam. The semi-logarithmic scale allows to appreciate the great difference in the scattering of light induced by these two kinds of texture.

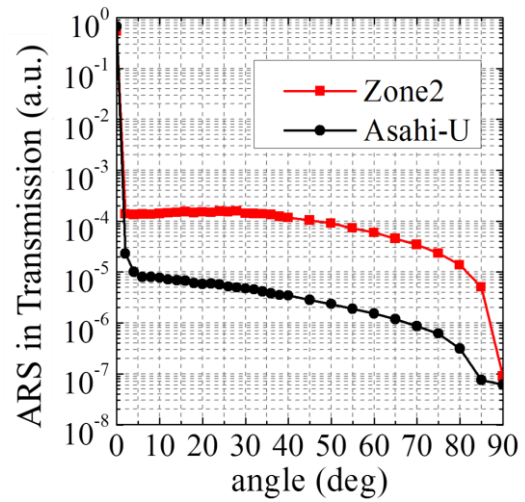


**Figure 6:** The graph of ARS in transmission at wavelength equal to 600 nm in absolute units. The data were divided by the intensity of the incident beam. The red curve (Zone2) is obtained on the sample with 150 nm RMS of texturing, while the black curve (Asahi-U) on 40 nm RMS. The semi-logarithmic scale allows to appreciate the great difference in the scattering of light performed by this two kinds of texture.

#### 3.4 Experimental setup for the haze

The haze is the ratio of the diffused component of the transmitted light over the total transmitted light as a function of wavelength. The measurement of haze gives the information on the fraction of the incident light which is scattered out of the specular direction. The measurement is done with an integrating sphere. To obtain the haze, the measurement is repeated twice: once by collecting all transmitted light and then by letting the specular component to go out from a little hole of the sphere. The ratio of the second to the first measurement gives the haze.

We use this technique to characterize the global scattering power of the textured sample on all the transmission half-space. We are interested in verifying if the one-dimensional rough sample remains a superior scatterer compared to the common Asahi-U substrate, when we consider scattering in all directions of transmission.

#### 3.5 Results for the haze

The characterization of scattering properties of the samples are completed by the haze measurements shown in Fig. 7. In red we report the haze measured on the best region (Zone 2) of the one-dimensional texture, while in black we show the haze measured on the common Asahi-U glass with SnO<sub>2</sub>.

We observe that the region centered on Zone2 of the 1D rough sample is characterized by a significantly larger haze compared to the Asahi-U texture. Interestingly, our sample is a stronger scatterer than the Asahi-U especially in the red and NIR ranges. These are exactly the ranges of interest for the realization of light-trapping in crystalline and micro-crystalline silicon thin-film solar cells.

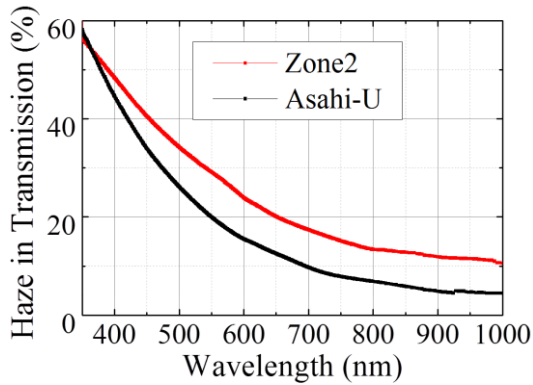


**Figure 7:** Ratio of the diffused component of the transmitted light on the total transmitted light (haze) as a function of the wavelength. Red curve (Zone2): haze measured on the best region of the one-dimensional texture. Black curve (Asahi-U): haze measured on the common Asahi-U  $\text{SnO}_2$  substrate with RMS equal to 40 nm.

#### 4 CONCLUSIONS

In this work we have investigated the scattering properties of pseudo-periodic one-dimensional glass nanostructures obtained by Ion Beam Sputtering. The proposed textured glass exhibits enhanced scattering properties with respect to the Asahi-U substrates commonly used in thin-film SCs. Moreover, a super-Lambertian behavior is observed in ARS measurements of the light transmitted through the sample.

Our next goal is to correlate the scattering properties of the rough glass/silicon interface with the photocurrent enhancement in thin-film SCs, conformally deposited on these substrates. Preliminary experiments performed using amorphous silicon thin-film SCs grown on the textured substrates show an improvement of the short-circuit current density ( $J_{sc}$ ) of the order of 15% with respect to cells grown on reference flat substrates [1]. Therefore, a greater improvement of  $J_{sc}$  is expected using crystalline or micro-crystalline silicon [4], as their lower band gap allows from a higher enhancement of absorption in the near-infrared spectral range.

#### ACKNOWLEDGEMENTS

The authors are grateful to Olindo Isabella for providing the Asahi-U sample and for helpful discussions.

#### REFERENCES

- [1] C. Martella et al, Nanotech. 24, 225201, 7pp (2013).
- [2] M. A. Green, Prog. Photovolt: Res. Appl. 10(4), pp 235-241 (2002).
- [3] P. Kowalczewski et al, Opt. Express. 21, No. S5, A808-a820 (2013).
- [4] C. Martella et al, J. Appl. Phys. 115, 194308 (2014).